International Journal of Applied Pharmaceutics

ISSN- 0975-7058 Vol 18, Issue 1, 2026

Original Article

BETULIN 3, 28-DIPHOSPHATE AS AN ACTIVATOR OF ANTIOXIDANT ENZYMES IN COMBINATION WITH AMINES AND AN ENHANCER OF BACTERICIDAL AND FUNGICIDAL ACTIVITY OF BENZALKONIUM CHLORIDE

NINA MELNIKOVA[1], DARINA MALYGINA[2*], IRINA KLABUKOVA[1], ANNA SOLOVEVA[3], ELENA AULOVA[1]

[1]The Faculty of Chemistry, the Lobachevsky State University, 23 the Gagarina Avenue, Nizhniy Novgorod-603950, Russia. [2]Department of Pharmaceutical Chemistry, Privolzhsky Research Medical University, 10/1 Minin Sq., Nizhniy Novgorod-603950, Russia. [3]Institute of Biology and Biomedicine, the Lobachevsky State University, 23 the Gagarina Avenue, Nizhniy Novgorod-603950, Russia

[*]Corresponding author: Darina Malygina; [*]Email: mds73@yandex.ru

Received: 25 Aug 2025, Revised and Accepted: 20 Oct 2025

ABSTRACT

Objective: The work was aimed to study properties of nanosuspensions of betulin diphosphate and its sodium salt in compositions with amines – trisamine, meglumine and benzalkonium chloride, for design of antioxidant medicines and enhance bactericidal and fungicidal activity of benzalkonium chloride.

Methods: This research work included the preparation and study of nanosuspensions. Nanoparticles formation was controlled using FTIR, UV and NMR spectrometry, PXRD, zeta-potential measurement and SEM visualization. Oxidoreductase activity was studied by specific activity of superoxide dismutase, catalase, glutathione reductase, glucose-6-phosphate dehydrogenase and aldehyde dehydrogenase. *Paecilomyces variotii*, *Aspergillus terreus*, *Penicillium chrysogenum*, *Staphylococcus aureus* and *Staphylococcus epidermidis* were used in study.

Results: Betulin diphosphate or its sodium salt in the presence of amines are capable of self-organization and formation of high positive charged nanoparticles (zeta potential from+37 to+51 mV) with various morphologic structures that allow to obtain transparent nanosuspensions.

Concentration of aged sodium salt of betulin diphosphate with amines was at least 0.644% that was higher than one of aqueous dispersions without amines. *In vitro* experiments on rat blood showed an increase in the specific activity of antioxidant enzymes under the action of all studied compositions. Sodium salt of betulin diphosphate showed synergetic effect of fungicidal and bactericidal properties of a known antimicrobial agent benzalkonium chloride in composition.

Conclusion: The revealed biological activity of new compositions of betulin diphosphate with amines can be useful in the treatment of various skin diseases.

Keywords: Betulin diphosphate, Trisamine, Meglumine, Benzalkonium chloride, Polymorphism, Antioxidant activity, Bactericidal and fungicidal properties

© 2026 The Authors. Published by Innovare Academic Sciences Pvt Ltd. This is an open access article under the CC BY license (https://creativecommons.org/licenses/by/4.0/)
DOI: https://dx.doi.org/10.22159/ijap.2026v18i1.56637 Journal homepage: https://innovareacademics.in/journals/index.php/ijap

INTRODUCTION

Poly-and solvatomorphism of betulinic acid and betulin is important, because their biological effects depend on structure [1-3]. The change in the physicochemical and biological properties of betulin and the appearance of its various polymorphic forms in the presence of glycine and PEG-4000 is an example of betulin isopolymorphism [4].

Recently, information has appeared on the effect of self-organization of betulin derivatives to form single-component nanoparticles that change the biological activity of the initial triterpenoid [5-9]. These structured nanosystems can both exhibit independent pharmacological activity and act as a delivery vector for other active pharmaceutical ingredients. An important direction in the creation of triterpenoid nanoparticles is the expansion of delivery options, not only oral and injection, but also endotracheal.

There are also known methods for improving bioavailability by incorporating triterpenoids, primarily derivatives of betulinic acid and betulin, into nanoparticles – liposomes, lipid nanoparticles with polymers, and others that are capable of dissolving in colloidal form at the required concentration [10-12].

A method for improving bioavailability has been proposed by various groups of chemists by functionalizing betulin derivatives with phosphate, phosphonate, or bisphosphonate groups at positions C-3, C-28, and C-(29-30) of the lupane skeleton [13-17]. Theoretical and experimental lipophilicity (logP from 6.937 to 7.982 for the most active compounds) have been reported and calculated for these compounds, although the correlation between lipophilicity and antitumor activity is more complex and ambiguous [15]. In general, it should be noted that, as a rule, the pharmacological action of betulin derivatives is improved by the inclusion of a phosphate group in the structure.

The concept of bioavailability may be more closely related to solubility for topical use of betulin derivatives. The betulin 3,28-diphosphate in pure form and in the form of salts with better solubility in water (from 0.1 to 5%) demonstrated *in vivo* and *in vitro* antitumor, anti-aggregation, antioxidant, hypolipidemic and other properties [18, 19]. The improved solubility of betulin 3,28-diphosate allowed its use for impregnation of wound dressings based on bacterial cellulose and as a component of hydrogels in the treatment of burn wounds.

The main problem of using betulin diphosphate in wide practice is the change of its physicochemical properties during storage (aging of the substance). A freshly prepared sample of Na-BDP in the hydrate form (Na-BDP·10H_2O) dissolved from 1 to 10%, in contrast to the aged sample (Na-BDP·(10-x)H_2O) with low solubility up to 0.1%. PXRD, FTIR spectroscopy, DSC and TG data proved crystalline structure of the initial highly soluble polymorph. During the storage desired crystalline polymorph transformed to a poorly soluble X-ray amorphous polymorph [18].

On the other hand, changes in solubility during aging and storage of triterpenoids can lead to a decrease in the bioavailability of these compounds, causing problems and difficulties in standardizing these compounds and development of effective dosage forms. One of the ways to improve the solubility of betulin diphosphate is complexation with amines such as dopamine, xymedone, trisamine, and meglumine [19]. The bioavailability of betulin diphosphate can also be caused by the association of betulin diphosphate with amine-containing components in solution, and the formation of transparent nanosuspensions with extremely small particle sizes. On the other hand, betulin diphosphate with an ionizable phosphate group can easily forms associates or salt complexes with organic cationic biocides such as benzalkonium chloride or Skulachev ions. Their

positively charged part interacts with the phospholipid bilayer of the bacterial cell membrane that leads to biocide penetration and membrane destabilization. These salt complexes containing a lipophilic anion with antioxidant properties and a cationic part of the biocide can significantly improve the bactericidal and fungicidal action.

In this work we studied the physicochemical and biological properties of betulin diphosphate and its sodium salt in compositions with amino alcohols – trisamine, meglumine, and benzalkonium chloride. We investigated: 1) the ability of betulin diphosphate and its sodium salt to form various polymorphic structures in the solid state; 2) the conditions for the formation of stable aqueous solutions or nanosuspensions in the liquid state and their properties; 3) the effect of the developed compositions on the specific activity of antioxidant defense enzymes; 4) the ability of sodium betulin diphosphate to exhibit synergism with benzalkonium chloride in bactericidal and fungicidal activity.

MATERIALS AND METHODS

Reagents

Trisamine ("Sigma Aldrich", 154565-100 G), meglumine (Merck, TD 13015143333) were purchased from Sigma-Aldrich, Russia, Moscow.

Betulin was purchased from "NPO Ecodika" (Kirov, Russia) and further purified by boiling with sodium hydroxide (0.5%) in toluene and recrystallized from ethanol or isopropanol. FTIR, ν, cm^{-1}: 3470 st (OH), 1640 st (C=C); ^{1}H NMR δ, ppm: 4.67 m (^{1}H, =CH_2), 4.57 m (^{1}H, =CH_2), 3.78 br. s (^{1}H, 28-CH_2OH), 3.31 m (^{1}H, 28-CH_2OH), 3.17 m (^{1}H, 3-CHOH), 2.36 m (^{1}H, 19-CH), 1.66 s (3H, CH_3), 1.23 s (3H, CH_3), 0.96 s (3H, CH_3), 0.94 s (3H, CH_3), 0.80 s (3H, CH_3), 0.74 s (3H, CH_3). ^{13}C NMR, δ, ppm: 76.71 (C-3), 109.46 (C-29), 150.24 (C-20), 57.87 (C-28).

Ethanol and benzalkonium chloride were purchased from Acros Organics, Russia, Moscow. Deionized water was obtained using deionizer Khromatek, Russia, Dzerzhinsk, the electrical conductivity was less than 0.1 μΩ/cm.

Betulin-3,28-diphosphate (BDP, 3β,28-diphosphate-lup-20(29)-ene) and the sodium salt of betulin-3,28-diphosphate were synthesized according to the procedure [18]. FTIR (KBr): ν_{max} 3421, 2331, 2342, 1641-1700, 1240, 1031, 973, 501 cm^{-1}; ^{1}H-NMR (DMSO-d_6, 400 MHz) δ 0.68–1.99 (42H, m, 6CH_3, $(CH_2)_{10}$, $(CH)_4$), 2.35–2.42 (1H, m, H-19), 2.97 (0.25H, wide t, α-H-3, *J* = 7.7 Hz), 3.69 (0.75H, ddd, β-H-3 m, *J* = 4.6, 7.8, 11.2 Hz), 3.96 (1H, dd, H-28, *J* = 9.7, 4.5 Hz) and 3.52 (H, dd, H-28′, *J* = 9.5, 4.5 Hz), 4.55, 4.69 (2H, two s, H-29), 5.69 (protons in the phosphate groups O-P(O)$(OH)_2$, wide blurred s); ^{13}C-NMR (DMSO-d_6, 101 MHz) *δ* 149.93 (C, C-20), 109.92 (CH_2, C-29), 82.96 (CH, =CHOH), 63.22 (CH_2, CH_2OH), 54.90 (CH, C-5), 49.71 (CH, C-9), 48.11 (CH, C-19), 47.26 (CH, C-18), 46.75 (C, C-17), 42.30 (C, C-14), 40.48 (C, C-8), 38.57 (C, C-4), 38.35 (CH_2, C-1), 37.99 (C, C-10), 37.07 (CH, C-13), 36.57 (CH_2, C-7), 33.79 (CH_2, C-22), 29.11 (CH_2, C-21), 28.96 (CH_2, C-16), 28.17 (CH_3, C-23), 27.90 (CH_2, C-2), 26.57 (CH_2, C-15), 24.83 (CH_2, C-12), 20.43 (CH_2, C-11), 18.84 (CH_3, C-30), 18.01 (CH_2, C-6), 16.14 (CH_3, C-26), 15.91 (CH_3, C-24), 15.70 (CH_3, C-25), 14.56 (CH_3, C-27); ^{31}P-NMR (DMSO-d_6, 202.46 MHz) δ −0.4 (d, *J* = 8.2 Hz, phosphoric acid residue at C-3β), 0.48 ppm (t, *J* = 4.6 Hz, phosphoric acid residue at C-28).

The sodium salt of betulin-3,28-diphosphate (Na-BDP) was obtained by adding 0.2–4.0 M aqueous alkaline (Na_2CO_3 or NaOH) solutions to aqueous or ethanol BDP solutions. FTIR (KBr) ν_{max} 3384, 2330, 1641–1700, 1375, 1089, 975, 513 cm^{-1}; ^{31}P-NMR (D_2O, 202.46 MHz) δ 4.25, 4.31 (d, *J* = 8.4 Hz, phosphoric acid residue at C-3β), 5.47 ppm (t, phosphoric acid residue at C-28).

Methods

FTIR spectra were obtained using a Fourier transform IR spectrometer IR Prestige-21 (Shimadzu, Kyoto, Japan), in KBr tablets.

UV spectra were recorded using a UV-1800 (Shimadzu USA Manufacturing Inc., Canby, OR, USA).

Powder X-ray diffraction patterns were obtained using an XRD-6000 X-ray diffractometer (Shimadzu, Kyoto, Japan) at 295(2) K with Cu Kα radiation (λ = 1.5418 Å) in the Bragg–Brentano reflection geometry. The samples were collected in the 2θ range between 5 and 50° with steps of 0.026° and 100 s of step size using a scan speed of 0.067335°/s. In the X-ray diffraction patterns of amorphous samples, there were diffraction peaks at 37.5° and 44.0°, which referred to the cuvette material.

Zeta potential was determined by phase analysis electrophoretic light scattering (PALS) on a NanoBrook Omni analyzer (Brookhaven Instruments, NY, USA). Before measurement, the cuvette was de-dusted by rinsing three times with deionized water. The Smoluchowski model was used by the software to convert electrophoretic mobility values into zeta potential values. All samples were 0.025% aqueous solutions.

^{13}C, ^{1}H and ^{31}P-NMR-spectra were obtained using a Jeol JNM ECX-400 spectrometer (Jeol Ltd., Tokyo, Japan), frequency 100, 400 and 202.46 MHz.

The morphology of the samples was obtained by scanning electron microscopy (SEM) on JSM-IT300LV (JEOL, Tokyo, Japan) with the electron probe diameter of about 5 nm and probe current below 0.5 nA (operating voltage 20 kV). The study of the sample surface topography was performed using the low-energy secondary electrons and backscattered electrons under low vacuum mode to eliminate charging.

Biological experiment

In vitro study of oxidoreductase activity. Male Wistar rats (200–250 g) were purchased from the Animal Breeding Facilities "Andreevka" Federal State Budgetary Institution of Science "Scientific Center for Biomedical Technologies" of the Federal Medical and Biological Agency (Andreevka, Moscow Oblast, Russia). The animal study was conducted according to the guidelines of the Declaration of Helsinki and approved by the Local Ethics Committee of Privolzhsky Research Medical University, Russian Federation (protocol no. 1 from 18 January 2021). All efforts were made to minimize animal suffering and to reduce the number of animals used. The rats were handled humanely, kept in plastic suspended cages, and placed in a well-ventilated and hygienic rat house under suitable room temperature (27±2 °C) and humidity conditions. They had unlimited access to food and water and were subjected to a natural photoperiod cycle of 12 h light and 12 h dark. The rats were in quarantine for two weeks before the study. All blood samples from the rats were performed under anesthesia. *In vitro* study was performed with blood samples stabilized with sodium citrate (1:9). Erythrocytes were washed twice with 0.9% NaCl by centrifugation for 10 min at 1600×g. Superoxide dismutase activity (EC 1.15.1.1) was measured in erythrocytes using inhibition of adrenaline auto-oxidation [20]. Catalase activity (EC 1.11.1.6) was determined by spectrophotometry based on the decomposition of hydrogen peroxide by the catalase [21]. Glutathione reductase activity (EC 1.8.1.7) was studied by spectrophotometry based on the oxidized glutathione reduction [22]. The activity of glucose-6-phosphate dehydrogenase (EC 1.1.1.49) was determined in hemolysate of erythrocytes by spectrophotometry based on glucose-6-phosphate oxidation to the phosphoglucolactone with the formation of reduced nicotinamide adenine dinucleotide phosphate (NADPH) [23]. The energy metabolism in erythrocytes was studied using the catalytic activity of LDH (LDH, EC 1.1.1.27), directly (LDH_{direct}, substrate – 50 mmol sodium lactate) and in reverse ($LDH_{reverse}$, substrate – 23 mmol sodium pyruvate) reactions [24]. The activity of aldehyde dehydrogenase (EC 1.2.1.3) was estimated spectrophotometrically in accordance with previous methods [25]. The specific activity of the enzymes was calculated from the protein concentration analyzed by the modified Lowry method [26].

The samples for the estimation of the biological activity were dissolved in phosphate buffer saline (PBS) using 2 μg/ml.

Antibacterial and fungicidal activity. Fungicidal activity was determined using three cultures (*Paecilomyces variotii*, *Aspergillus terreus*, *Penicillium chrysogenum*). The samples are infected with mold spores in a solution of mineral salts with the addition of sugar (Czapek-Dox medium). The samples were placed in wells on agarized Czapek-Dox medium in sterile Petri dishes. Then the surface of the sample and the medium were inoculated with a spore suspension of individual test cultures of

micromycetes and the Petri dishes with the samples were placed in a thermostat. The test duration was 14 d at a temperature of 29±2 °C and humidity>90%. The samples had fungicidal properties if an inhibitory zone (zone of no fungal development) was observed around the sample on the nutrient medium.

The bactericidal properties were assessed using *Staphylococcus aureus* and *Staphylococcus epidermidis* cell cultures by the size of the zone of inhibition of bacterial growth around the studied samples placed in wells on the meat-peptone agar medium. The test duration was 24 h at a temperature of 37 °C.

Statistical analysis

Statistical data processing was performed by the software (Statistica 6.0 (StatSoft Inc., Tulsa, OK, USA)). The normality of a distribution of results was shown using the Shapiro-Wilk test. The significance of differences between groups was assessed using Student's t-test. The differences were considered statistically significant at $p<0.05$.

RESULTS AND DISCUSSION

Determination of stability and aging conditions on the base of physical and chemical properties of betulin 3,28-diphosphate and its sodium salt is important to design amine-containing antioxidant compositions for skin diseases treatment. The bactericidal and fungicidal composition was developed based on betulin diphosphate sodium salt and benzalkonium chloride (BC).

Interaction of BDP with amino alcohols in aqueous-alcoholic solutions

For the study, a 1% alcohol solution of BDP and aqueous solutions of amino alcohols were used to obtain mixed aqueous-alcoholic compositions at an alcohol-water ratio of 1:1 and a molar ratio of BDP: amino alcohol equal to 1:2 or 1:4.

When trisamine interacted with BDP in an aqueous-alcoholic solution at a molar ratio of BDP: trisamine = 1:4, the mixture initially was a cloudy milky solution. Within a week, a precipitate in the form of spherical particles was formed (fig. 1a).

After separation of the supernatant, the precipitate in the form of spherical particles was homogenized with a small amount of water. Within a week, an aqueous-alcoholic gel was formed (fig. 1b). Over time, granules were formed in the supernatant (fig. 1c), the shape and size of which depended on the conditions. At lower temperatures, the smaller granules were formed more intensively (fig. 1d). The appearance of the precipitates is like that of polyphosphate surfactants, which tend to self-organize into ball-like structures.

Unlike trisamine, meglumine formed a transparent solution when interacting with BDP, which did not form a gel under similar conditions. Initially, the yellow-green color of the solution appears in the system. The crystalline salt isopolymorph of BDP of a greenish tone slowly forms from this solution (fig. 1e) with the subsequent formation of a greenish powder (fig. 1f).

To illustrate the formation of isopolymorphic structures of BDP in the composition, we studied a mixture of BDP and benzalkonium chloride with cationic ammonium fragment. When mixing BDP with benzalkonium chloride, a light suspension was initially formed, and after evaporation of the solvent, a thick lemon-yellow resin was formed, while the precipitate did not crystallize over time (fig. 1g).

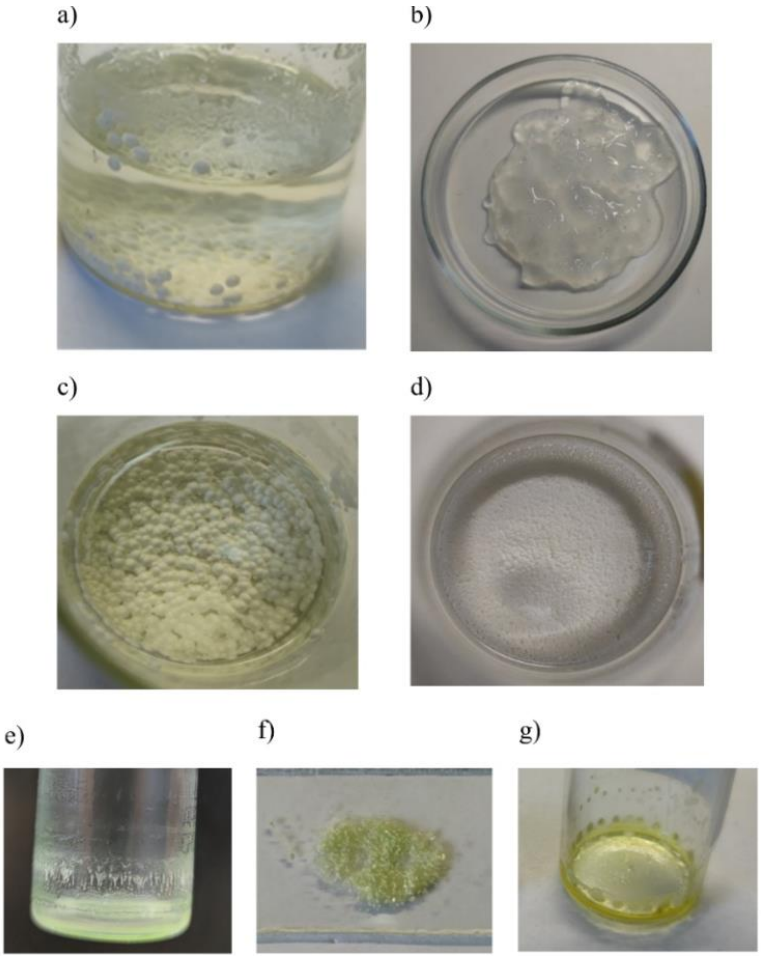

Fig. 1: Photo of BDP-trisamine (1:4) composition: a) one week after mixing; b) gel formed by the precipitate upon addition of water; c) after 2 w in the supernatant at room temperature; d) after 2 w in the supernatant at+8 °C. BDP-meglumine (1:4) composition: e) one week after mixing (formation of crystals); f) greenish powder after air drying; g) BDP-benzalkonium chloride (1:4) system

It was shown that the differences in the properties of products with different molar ratios were insignificant, and further results of the work are presented only for the ratio 1:4.

The ^{31}P-NMR data of the analyzed samples in the BDP-trisamine (1:4) and BDP-meglumine (1:4) systems show minor changes in the phosphorus signals at the C-28 and C-3 atoms to a more polar region relative to the ^{31}P-NMR spectrum of BDP (table 1, fig. 2, fig. 3). Chemical shifts of BDP-meglumine (1:4) were 1.68 ppm and 0.63 ppm, ones of BDP-trisamine (1:4) were 1.10-1.12 ppm and 2.10 ppm, ones of BDP were 0.25 ppm and-0.65 ppm for C_{28}-P and C_3-P atoms, correspondingly. Moreover, the chemical shifts of the sodium salt of BDP in DMSO do not differ from those of BDP.

An exception is the BDP-BC (1:4) sample obtained from an aqueous-alcoholic solution in the form of a green resin. The phosphorus atom at C-28 (-0.95 ppm) becomes less polar compared to the phosphorus atom at C-28 of the initial BDP (0.25 ppm). It can be assumed that the negatively charged phosphate group of BDP interacts with the cationic ammonium fragment of BC, forming an ionized complex or chelate that is better soluble in water than the initial BDP.

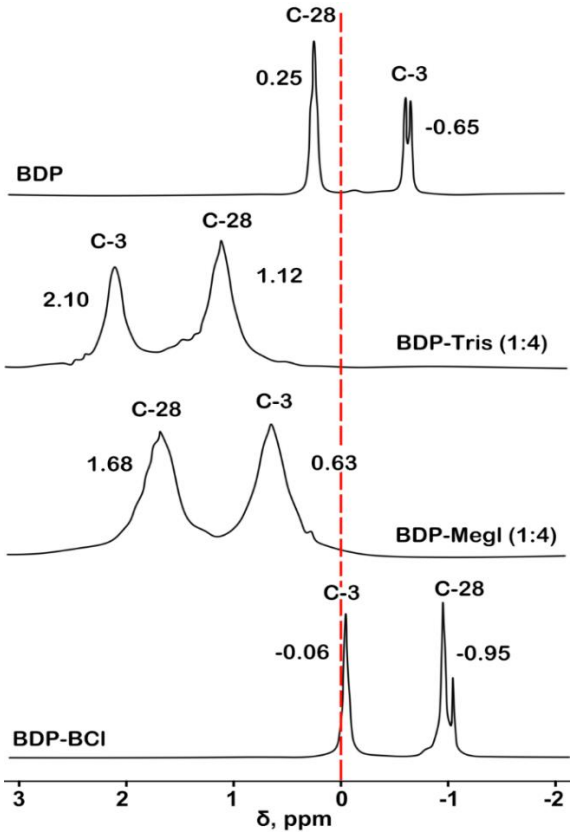

Fig. 2: ^{31}P-NMR spectra of BDP solutions (a); BDP-trisamine (1:4) from round spherical particles (b); crystalline precipitate of BDP-meglumine (1:4) obtained from an aqueous-alcoholic solution (c); green resin formed from an aqueous-alcoholic solution of BDP-BC (1:4) (d). Solvent – DMSO-d6, standard – Ph_3P

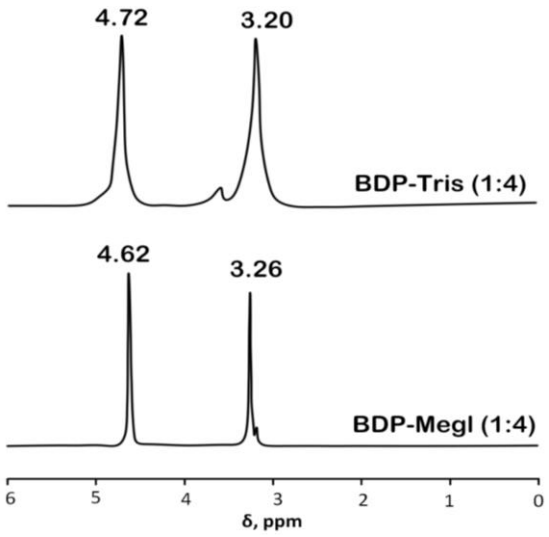

Fig. 3: ^{31}P-NMR spectra of solutions of the crystalline precipitate BDP-trisamine (1:4), obtained from a water-alcohol solution (top); BDP-meglumine (1:4) from round spherical particles (bottom). Solvent – D_2O, standard – phosphoric acid

Table 1: Data of ^{31}P-NMR spectra

Sample	Solvent	Chemical shift δ, ppm	
		C_{28}-P	C_3-P
BDP (initialpowder)	DMSO-d6	0.25	-0.65
BDP-trisamine (1:4) from dried gel		1.10	2.10
BDP-trisamine (1:4) from granulated sediment		1.12	2.10
BDP-meglumine (1:4), a crystalline precipitate obtained from an aqueous-alcoholic solution		1.68	0.63
BDP-BC (1:4), green resin formed from a water-alcohol solution		-0.95	-0.06
BDP-trisamine (1:4)	D_2O	4.72	3.20
BDP-meglumine (1:4)		4.62	3.26

The FTIR spectral data represent a superposition of bands with overlapping bands of amines and BDP (in close wavenumber intervals). In the spectra of the salt complexes BDP-trisamine (1:4) and BDP-meglumine (1:4), obtained as a dry gel, stretching vibrations of OH and NH_2 groups were observed in the region of 3500-3400 cm^{-1}, stretching vibrations of the triterpenoid and amino alcohol skeletons (2944-2866 cm^{-1}), stretching vibrations of alcohol νC-O (trisamine) and ether groups of phosphoric acid νC-O and νP-O (BDP) in the region of 1049-1059 and 972 cm^{-1}. The spectrum clearly shows the stretching vibrations of the polar phosphate group in the region of 517 cm^{-1}, νP=O in the region of 1374 cm^{-1}.

The UV spectra of all analyzed compositions had a smoother and less intense absorption band in the region of 245-295 nm, in contrast to the UV spectra of the initial BDP, which has several absorption bands due to the phosphate group.

Therefore, studying water-alcohol reaction mixtures (FTIR, NMR, UV) and the appearance of precipitates from them, it can be assumed that BDP can form various polymorphic forms with amines. It is probably due to the stabilization of phosphate groups in the form of α-epimers by complexes formation. Subsequently, we used the ionized form of BDP in the form of sodium salt to stabilize BDP compositions with amines.

Interaction of Na-BDP with amino alcohols in aqueous-alcoholic solutions

Na-BDP compositions with amino alcohols (meglumine and trisamine) were obtained similarly to compositions with BDP, using a 1% Na-BDP solution in a water-alcohol medium as the initial solution, with a Na-BDP: amino alcohol ratio of 1:2 and 1:4. Aged Na-BDP·(10-x)H_2O samples were used to standardize the experimental conditions, which did not subsequently change their structure and solubility. Table 2 shows the solubility data of the main studied components.

In all cases, transparent solutions were initially formed when obtaining the Na-BDP composition with amino alcohols.

Table 2: Solubility of BDP, Na-BDP and their combinations with amino alcohols

N	Sample	Solubility, % (solvent)
1	Na-BDP·10H_2O (fresh prepared)	10.02 (H_2O)
2	Na-BDP·(10-x)H_2O (after 6 mo storage)	0.51 (H_2O)
3	BDP (freshprepared)	1.00 (water-alcohol)
4	BDP-meglumine (1:4)	0.50 (water-alcohol)
5	BDP-trisamine (1:4)	0.50 (water-alcohol)
6	BDP-BC (1:2)	1.00 (water-alcohol)
7	Na-BDP·(10-x)H_2O-meglumine (1:4)	0.64 (H_2O)
8	Na-BDP·(10-x)H_2O-trisamine (1:4)	0.64 (H_2O)
9	Na-BDP·(10-x)H_2O-BC (1:2)	0.64 (H_2O)

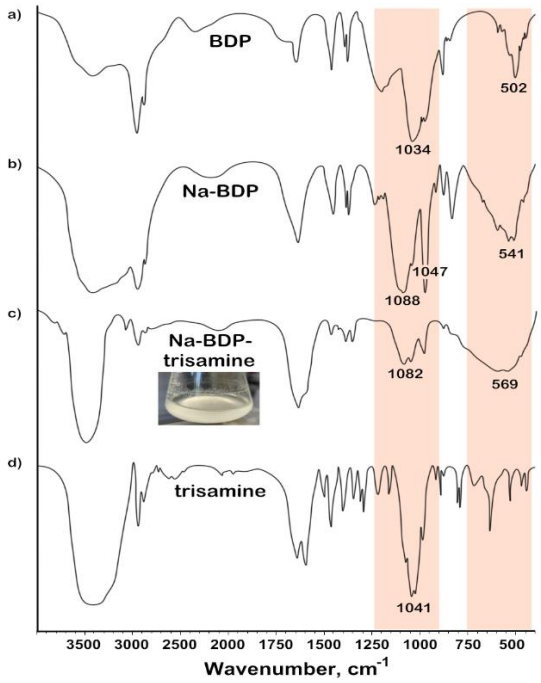

Fig. 4: FTIR spectra of samples: a) BDP; b) Na-BDP; c) Na-BDP-trisamine (4:1); d) trisamine

After a week, a light suspension was formed in the solutions at the bottom and thin needle-like crystals were formed above the liquid level on the walls of the flask. The FTIR spectra of the isolated crystalline precipitates were clearer than the compositions isolated from mixtures of amino alcohols with BDP (fig. 4 and 5).

The shape and position of the stretching vibration bands of the C-O alcohol groups in trisamine (ν 1041-1022 cm^{-1}) and C-O ester groups (ν 1031-973 cm^{-1}) in BDP were changed to a broad band in the region of 1070-970 cm^{-1}. The stretching vibrations of P-O (ν 497 cm^{-1}) and P=O (δ 1641 cm^{-1}, δ 1215 cm^{-1}) of BDP were significantly changed. The band around 1641 cm^{-1} can also be attributed to the bending of the H–O–H bonds of hydrated water molecules, as indicated in [27] for manganese phytate. In [28], the fine structure of these bands was explained by the presence of infrared overtones of the normal modes δ(PO–H) and ρ(PO–H). In the FTIR spectra of phytates, the intense and broad band observed between 1250 and 700 cm^{-1} for salt complexes is associated with several normal modes of phosphate groups.

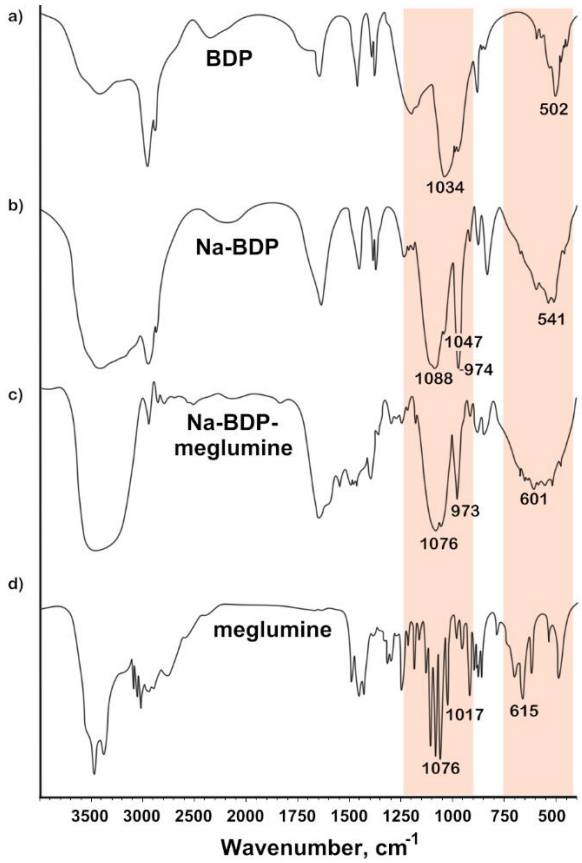

Fig. 5: FTIR spectra of samples: a) Na-BDP; b) Na-BDP-meglumine (4:1); c) meglumine

This band splits into three peaks upon complexation and deprotonation [29]. The first two bands around 1088 and 1047 cm^{-1} are due to the asymmetric and symmetric stretching of the PO_2^- groups. In fact, these two bands have already been described for pyridoxal phosphate [30]. The third band is in the region of 973 cm^{-1} can be associated with ν(P–OH) and ρ(PO–H) vibrations for Na-BDP and its salt complexes with trisamine and meglumine, it is consistent with data obtained for some other complexes [31]. Finally, the band at 541-601 cm^{-1} in the spectra of the studied substances is due to the normal mode δ(O–P–O). The splitting and shifting of bands associated with phosphate vibrations is a sign of direct and bidentate coordination of O-P with the cation [32, 33].

In general, changes in the FTIR absorption spectra of pure Na-BDP and Na-BDP in compositions with amines (significant broadening and change of bands in the regions of 502-601 cm^{-1} and 1630 cm^{-1}, change of band in the region of 3400 cm^{-1}) can be caused by the formation of associative structures characteristic of nanoparticles. Similar situation was observed for betulinic acid nanoparticles in the work [9].

The obtained results on solubility can probably be explained by the similarity of the conformational structure of betulin diphosphate, betulin and betulinic acid by the position of the polar group at C-3. The low solubility of betulin and betulinic acid is primarily due to the stability of their β-epimers at position C-3 (β-OH) in the chair conformation of cyclohexane rings. β-OH epimers with the equatorial position of the hydroxyl group promote strong hydrophobic binding and weak binding due to hydrogen forces, which leads to the low solubility of these compounds [34]. Betulin 3,28-diphosphate is initially formed as a mixture of α-and β-epimers of the phosphate groups [18], and the freshly prepared sample is more soluble in water. In the ^{13}C-NMR spectra and ^{13}C-DEPT spectra, two signals of the BDP C-3 atom are observed with a difference of 0.06 ppm (6.25 Hz), while old sample has only one signal. The two epimers had different ^{1}H-NMR resonance values of H-3 (fig. 6): δ = 2.97 ppm for α-H-3 (broad triplet, J = 7.7 Hz) and δ = 3.69 ppm for α-H-3 (broad triplet, J = 7.7 Hz). For β-H-3 (ddd, J_1 = 4.6 Hz, J_2 = 7.8 Hz, J_3 = 11.2 Hz). ^{1}H-NMR resonances of H-28 were observed in the region of 3.96 ppm (H-28, dd, J_1 = 9.7 Hz, J_2 = 4.5 Hz) and 3.52 ppm (H-28′, dd, J_1 = 9.5 Hz, J_2 = 4.5 Hz).

The effect of the stereochemistry of pure triterpenoids and their complexes with amines on nanoparticle stabilization and the reduction in the rate of aging, which leads to decrease in solubility, may be due to changes in molecular conformation. The interaction of triterpenoids with amines promotes the transition of the stable, poorly soluble β-epimer to the more readily soluble α-epimer. These assumptions are also supported by the ^{1}H-NMR spectra of the starting triterpenoids and their reaction products with amines (fig. 7).

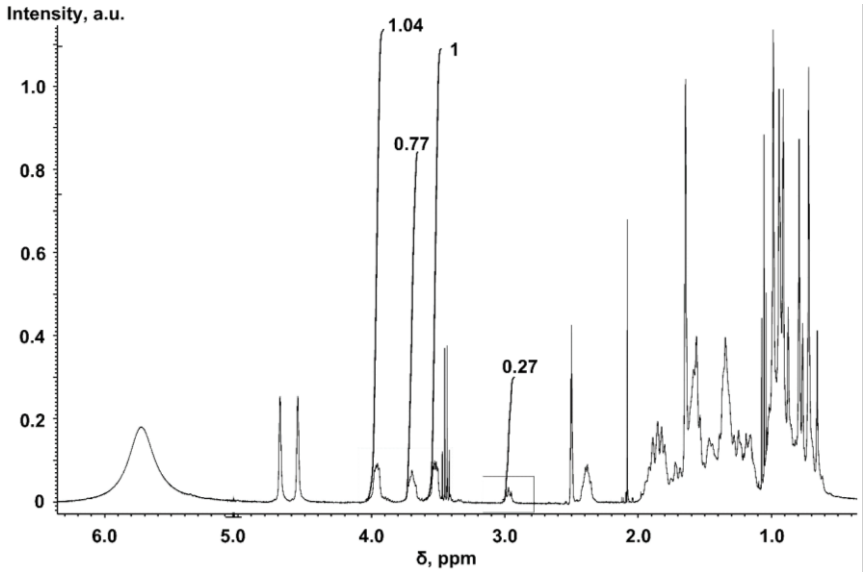

Fig. 6: General ^{1}H-NMR spectrum of BDP and Na-BDP. Solvent – DMSO-d6, standard –TMS

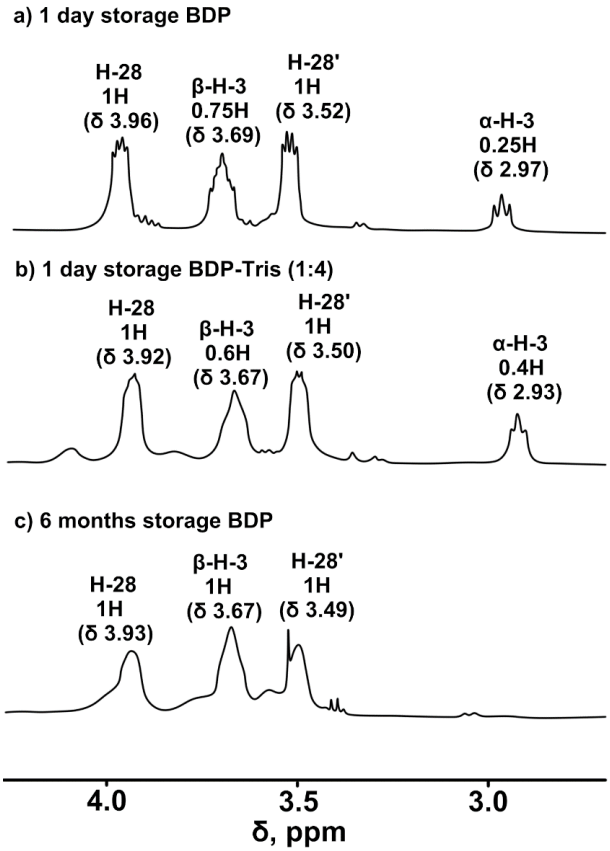

Fig. 7: ^{1}H-NMR spectra of a) BDP or Na-BDP after 1 day of storage; b) BDP-trisamine (1:4); c) BDP or Na-BDP after 6 mo of storage. Solvent – DMSO-d6, standard –TMS

Freshly prepared triterpenoids (usually in the form of hydrates) are more soluble in water and predominantly represent the α-epimer. Over time, with changes in the amount of hydration water, a transition to the β-epimer is observed at a β-epimer to α-epimer ratio of 75% to 25%. At the same time, the solubility of both BDP and the sodium salt of BDP decreases. The products of interaction with amines can increase the proportion of the α-epimer and, consequently, improve solubility. ^{1}H-NMR spectra confirm these conformational transitions. This process of self-organization was enhanced in the cold (+8 °C) at a higher concentration of ethanol, and after evaporation of the solvent, round ball-like particles of 1-2 mm in diameter were formed.

Lyophilic drying of aqueous or aqueous-alcoholic nanosuspensions (solutions) allows to obtain various crystalline polymorphic forms of complex compounds (fig. 8).

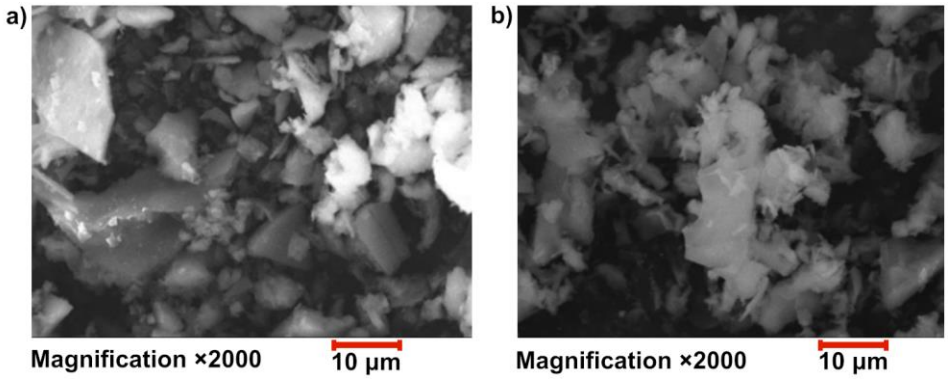

Fig. 8: SEM visualization of powder of compositions after freeze drying: (a) Na-BDP: trisamine (1:4); (b) Na-BDP: meglumine (1:4). Magnification ×2000

X-ray diffraction patterns of the isolated precipitates of Na-BDP salt complexes with trisamine 1:4 and 1:2 demonstrated partial preservation of the crystal structure of the initial Na-BDP (fig. 9 and 10), but broadening of the signals was noted, especially in the region of small Bragg angles 2θ from 10° to 15°.

With a decrease in the proportion of amine (1:2), this broadening in the form of a hump on the X-ray diffraction pattern is more clearly visible. A similar picture is observed for Na-BDP isopolymorphs in compositions with meglumine. At the same time, at a ratio of 1:2, an X-ray amorphous structure characteristic of amorphous nanoparticles was observed. The results obtained by us on PXRD analysis are close to the results on X-ray diffraction patterns of amorphous nanoparticles of betulinic acid [9].

Dried powders of Na-BDP compositions with amines were dissolved in water to obtain a transparent solution with a concentration of 0.025% to evaluate the zeta potential of the resulting nanoparticles. It was shown that the solutions of all compositions had the form of stable nanosuspensions and were characterized by large positive values of zeta potential from+37 to+51 mV (table 3).

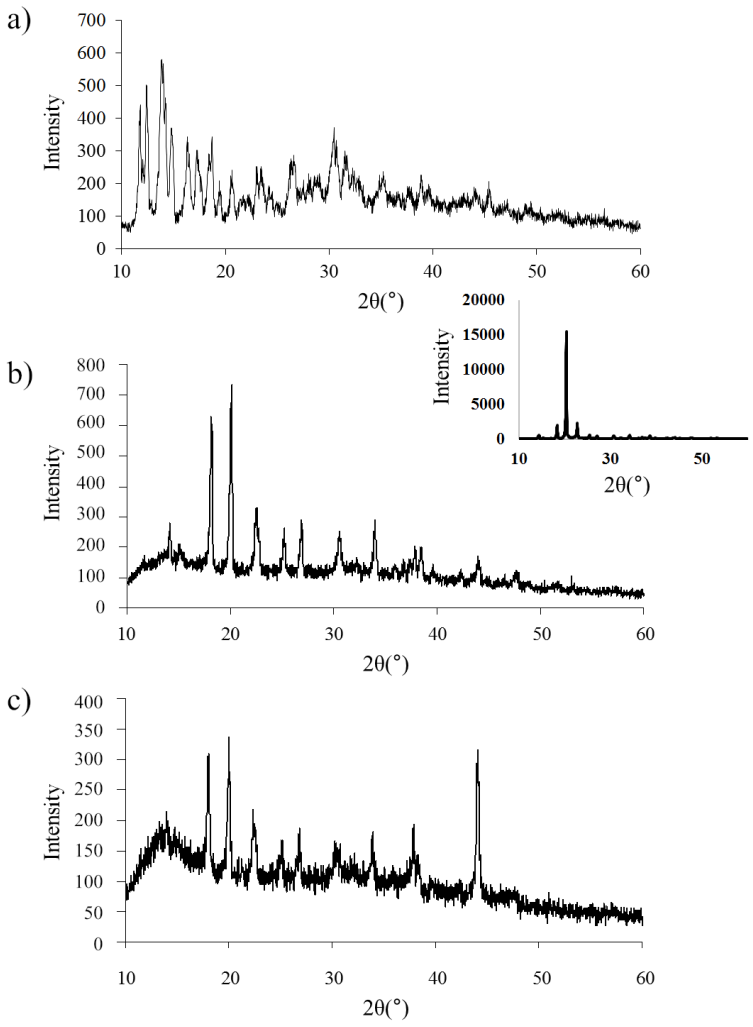

Fig. 9: X-ray diffraction patterns of Na-BDP (top), Na-BDP-trisamine (1:4, center) and Na-BDP-trisamine (1:2, bottom). Insert – trisamine. Diffraction peaks at 37.5° and 44.0° referred to the cuvette material

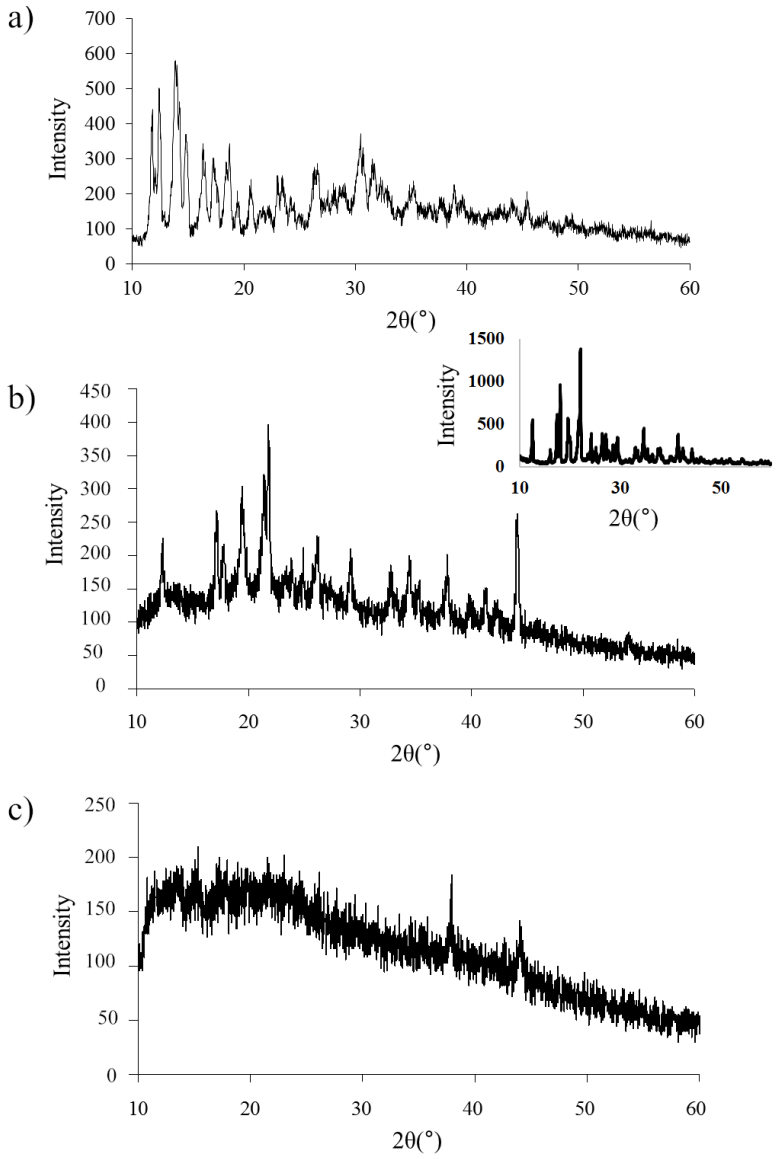

Fig. 10: X-ray diffraction patterns of BDP-Na (top), BDP-Na-meglumine (1:4, center) and BDP-Na-meglumine (1:2, bottom). Insert – meglumine. Diffraction peaks at 37.5° and 44.0° referred to the cuvette material

Table 3: UV spectral data and zeta potential measurement results for Na-BDP compositions with amino alcohols

Sample	Wavelength, nm	Absorbance	Zeta potential, mV
Na-BDP-trisamine (1:4)	291.00	0.276	+44.87±3.00
Na-BDP-meglumine (1:4)	291.00	0.228	+37.24±1.44
Na-BDP-trisamine (1:2)	291.00	0.339	+51.53±1.18
Na-BDP-meglumine (1:2)	287.00	0.291	+42.21±2.09

At the same concentration of Na-BDP in the solution, the appearance of the UV spectra (both the position of the band and the absorption maximum) differed and a bathochromic shift from 256 nm (initial Na-BDP) to 291 nm was observed (table 3).

The values of zeta potentials, along with the data of X-ray diffraction patterns, broadening of bands in the IR spectra, shifts of bands in the UV spectra, similar to betulinic acid nanoparticles [9], confirm the X-ray amorphous structure of Na-BDP nanoparticles and its compositions with amines. Considering the advantages of betulinic acid nanoparticles in increasing bioavailability and biological activity compared to the initial poorly soluble betulinic acid, it can be assumed that Na-BDP nanoparticles obtained in compositions with amino alcohols can also improve their pharmacological properties compared to the initial Na-BDP, which undergoes to aging.

Action of aqueous nanosuspensions of Na-BDP compositions with meglumine and trisamine (1:4) nanoparticles, which do not change their physicochemical properties during storage, on the specific activity of first-line antioxidant defense enzymes (SOD, catalase, glutathione reductase and glucose-6-phosphate dehydrogenase activities, ALDH, LDH) was studied at a dose of 2 μg/ml (table 4). These results on specific enzyme activity compared to intact rat blood showed that superoxide dismutase (SOD) activity increased by 2-3 times, catalase – by 1.2-1.8 times, glutathione reductase (GR) – by 1.5-2.0 times, glucose-6-phosphate dehydrogenase (G6PD) – by 1.2-2.0 times, aldehyde

dehydrogenase (AlDH) – by 1.2-2.2 times. Lactate dehydrogenase (LDH) specific activity increased by 1.6-2.3 times in direct reactions and up to 1.4 times in reverse reaction. The increase on specific enzyme activities of compositions from freeze-dried Na-BDP compared to ones of crystalline sample of Na-BDP after 6 mo of storage was approximately 1.3-1.7 times (table 4).

Activation of antioxidant enzymes leads to a reduction in oxidative stress in the body and promotes wound healing by reducing inflammation. It can be assumed that the Na-BDP-amino alcohol composition containing nanoparticles obtained by lyophilization with a high zeta potential in aqueous nanosuspensions (+37-+51 mV) is capable of more effectively activating antioxidant enzymes.

Development of Na-BDP nanoparticles composition with antibacterial and fungicidal action

Despite the fact that all aqueous solutions of Na-BDP mixtures with benzalkonium chloride at a concentration of up to 1% Na-BDP at a molar ratio of 1:0.1 to 1:4 in water were transparent and stable for 6 mo, their zeta potential was high (+51.34±3.19). This fact characterizes the formation of ultra-small positively charged nanoparticles in an aqueous solution of Na-BDP, even with an insignificant content of benzalkonium chloride. BDP has proven itself as an effective component of wound healing agents, accelerating the healing of burn wounds, causing an acceleration of skin regeneration processes, positively influencing the synthesis of collagen.

Table 4: Biochemical indexes (SOD, catalase, glutathione reductase and glucose-6-phosphate dehydrogenase, aldehyde dehydrogenase, lactate dehydrogenase in direct and reverse reactions activities) of BDP-Megl and BDP-Tris mixtures. Molar ratio of BDP: amine is 1:4. Data are presented as mean±SD (n = 5 biologically independent samples)[a,b,c]

Sample	Na-BDP sample preparation conditions	Index, % of control						
		SOD	Catalase	GR	G6PD	AlDH	LDH_{dir}	LDH_{rev}
Na-BDP	From a crystalline sample of Na-BDP after 6 mo of storage	226.18± 14.92*	116.03± 10.89	142.54± 12.89*	121.64± 13.45	119.63± 7.73	161.42± 15.75*	106.09± 6.05
	From freeze-dried Na-BDP	301.94± 10.34*	146.47± 14.63*	205.24± 11.60*	153.05± 6.75*	144.64± 17.79*	212.69± 12.27*	126.15± 16.10
Na-BDP-MeglumineNPs (1:4)	From freeze-dried Na-BDP	329.97± 16.52*	168.61± 6.12*	219.44± 4.16*	208.71± 9.26*	201.31± 10.61*	213.53± 17.39*	138.88± 12.66*
Na-BDP-Trisamine NPs (1:4)	From freeze-dried Na-BDP	351.62± 19.02*	179.29± 8.96*	217.19± 8.59*	204.86± 11.87*	219.29± 19.51*	229.17± 9.36*	128.02± 15.55

[a]Biochemical indexes values are taken as 100%; superoxide dismutase (SOD) – 846.24 Ru/mg protein; catalase – 31.66 Ru/mg protein; glutathione reductase (GR) – 91.48 nmol NADH/(min·mg protein); glucose-6-phosphate dehydrogenase (G6PH) – 54.17 nmol NADPH/(min·mg protein); aldehyde dehydrogenase (AlDH) – 22.02 nmol NAD^+/(min·mg protein); lactate dehydrogenase in direct reaction (LDH_{dir}) – 21.86 nmol NAD^+/(min·mg protein); lactate dehydrogenase in reverse reaction (LDH_{rev}) – 172.54 nmol NADH/(min·mg protein). [b]Concentration was calculated by Na-BDP. c*differences are statistically significant compared to the control ($p<0.05$).

Our experiments showed that neither Na-BDP nor its complexes with meglumine exhibit fungicidal and bactericidal properties (tables 5 and 6).

In this context, Na-BDP nanoparticles in compositions with a small amount of benzalkonium chloride can contribute to antimicrobial and fungicidal properties, which is extremely important in wound healing products. Benzalkonium chloride is effective against a number of micromycetes that are not affected by Na-BDP.

Benzalkonium chloride's mechanism of action involves membrane destabilization, leading to cell lysis and leakage of intracellular components, which leads to the death of bacterial and fungal cells [35-37]. Similarly, under the influence of BC, destabilization of the membrane of the bacterial cell of *Staphylococcus aureus* and *Staphylococcus epidermidis* occurs, causing various skin infections, sepsis and purulent infection of wounds. It should be assumed that the lipophilic component – betulin diphosphate with an ionizing phosphate group, in combination with the cationic part of benzalkonium chloride, can improve the penetration and destabilization of the cell membrane. Tables 5 and 6 show that the composition of Na-BDP with benzalkonium chloride significantly improved the fungicidal action in the case of *Aspergillus terreus*, *Penicillium chrysogenum* and *Paecilomyces variotii* and bactericidal action in the case of *Staphylococcus epidermidis* compared to benzalkonium chloride. The bactericidal activity against *Staphylococcus aureus* for the composition of Na-BDP with benzalkonium chloride did not differ significantly from the activity of pure benzalkonium chloride, but was also higher.

The synergism of the biocidal and fungicidal action of Na-BDP and BC in the composition may be due to the positive effect of the lipophilic ionizable fragment of the phosphate group of Na-BDP on the mechanism of BC action at all stages of exposure to the cytoplasmic membrane. The lipophilic diphosphate fragment improves the adsorption and penetration of BC through the cell wall with a subsequent reaction with the cytoplasmic membrane (lipid or protein), with subsequent disorganization of the membrane, which leads to leakage of intracellular material with a lower mass, degradation of proteins and nucleic acids and lysis of the cell wall caused by autolytic enzymes. The enhanced action and synergistic effect of the triterpenoid can be explained by the extremely high positive charge of the nanoparticles in the nanosuspension (zeta potential of+40-+50 mV) along with the positively charged benzalkonium chloride cation. A number of studies have shown that the positive charge of nanoparticles more effectively affects the adsorption capacity of bacteria with negatively charged cell walls [38, 39].

Table 5: Fungicidal activity of benzalkonium chloride with Na-BDP combinations. The test duration was 14 d at a temperature of 29±2 °C and humidity>90%. Data are presented as mean±SD (n = 5 biologically independent samples)

Micromycetes	Degree of material overgrowth with micromycetes	Sample composition, %		
		benzalkonium chloride 1,5	Na-BDP 0.644 Meglumine 0,390	Na-BDP 0.644 benzalkonium chloride 0,375
Aspergillus terreus	Degree[a]	0	5	0
	Zone of inhibition of fungal growth, mm	14.20±1.79	0	20.40±2.88*
	Effect	fungicidal	non-fungicidal	fungicidal
Penicillium chrysogenum	Degree	0	5	0
	Zone of inhibition of fungal growth, mm	13.40±2.41	0	19.20±2.17*
	Effect	fungicidal	non-fungicidal	fungicidal
Paecilomyces variotii	Degree	0	5	0
	Zone of inhibition of fungal growth, mm	41.20±3.70	0	50.80±3.70*
	Effect	fungicidal	non-fungicidal	fungicidal

[a]Intensity of fungal growth on a five-point scale, *The differences are statistically significant compared to benzalkonium chloride ($p<0.05$)

Table 6: Bactericidal activity of benzalkonium chloride with Na-BDP combinations. The test duration was 24 h at a temperature of 37 °C. Data are presented as mean±SD (n = 5 biologically independent samples)[a]

Sample composition, %	Zone of bacterial growth inhibition, D = mm			
	Staphylococcus aureus	Effect	*Staphylococcus epidermidis*	Effect
benzalkonium chloride 1,5	23.80±3.56	strongly bactericidal	17.40±2.30	bactericidal
Na-BDP 0.644	-	non-bactericidal	-	non-bactericidal
Meglumine 0,390				
Na-BDP 0.644	27.60±2.79	strongly bactericidal	24.20±2.59*	strongly bactericidal
benzalkonium chloride 0,375				

[a]"-"means no zone of bacterial growth inhibition, *The differences are statistically significant compared to benzalkonium chloride ($p<0.05$)

In this regard, micromycetes that are destroyed by benzalkonium chloride were used in the work – *Paecilomyces variotii*, *Aspergillus terreus*, *Penicillium chrysogenum*. *Aspergillus terreus* can cause mycosis of the skin, otomycosis, onycomycosis, mycotoxicosis, upper respiratory tract infections, allergies; *Penicillium chrysogenum* causes mycosis of the spleen, kidneys, heart, skin; ear inflammation, lesions of the tongue and eyes; mycotoxicosis, allergies; *Paecilomyces variotii* causes paecilomycosis of the lymph nodes, glands, upper respiratory tract (sinusitis), organs of vision, mycotoxicosis, allergies.

The antioxidant properties of Na-BDP and its high lipophilicity in the form of nanoparticles can be effective when acting on the above-mentioned micromycetes and bacteria.

Therefore, Na-BDP-BC, with a fungicidal effect against fungi, some strains of which can cause various mycoses, and a bactericidal effect against bacterial causative agents of skin infections *Staphylococcus aureus* and *Staphylococcus epidermidis*, can be used for the treatment of skin diseases.

The problem of low solubility and, accordingly, bioavailability of natural compounds – triterpenoids of the lupane group, is acute for the pharmaceutical industry, despite their high biological activity proven in experiments and in practice. Often, difficulties in the development of drugs are associated with solvato-, poly-and isopolymorphism of these compounds, arising in a certain production and over time, which is most clearly shown by the example of betulin, betulinic acid and their derivatives. In this regard, problems of standardization of substances arise, and well-developed formularies of drugs can lose their pharmacological activity over time.

The results of this work showed the effect of various amines on the example of two amino alcohols (trisamine and meglumine) and quaternary ammonium salt benzalkonium chloride on the physicochemical and antioxidant properties of polymorphs of 3,28-diphosphate of betulin and its sodium salt. Moreover, the ability of betulin diphosphate to form various polymorphic forms with amino alcohols due to the association of molecules by the phosphate group bound to amino alcohols was shown using the data of the solubility study, FTIR, UV, NMR spectral methods.

CONCLUSION

Problem of lower solubility of betulin diphosphate and its sodium salt in water is dependent on aging of these substances during storage. The solubility of betulin diphosphate and its sodium salt can be improved due to formation of compositions with amines (trisamine, meglumine and benzalkonium chloride) in the ratios 1:2 and 1:4. When storing aqueous-alcoholic dispersions of the compositions in the presence of amines, the formation of gel structures, spherical granules and crystals is possible. Sodium salt of BDP is capable of forming transparent solutions or nanodispersions in the presence of all the studied amines – trisamine, meglumine and benzalkonium chloride, in the concentration range from 0.1% to 0.6%. Freeze-drying of aqueous or aqueous-alcoholic nanosuspensions leads to various crystalline structures formation. Powder X-ray diffractometry has proven the existence of crystalline Na-BDP in the form of nanoparticles with large positive value of the zeta potential (+37-+51 mV).

Na-BDP compositions with meglumine, trisamine and benzalkonium chloride did not change their properties during long-term storage and demonstrated high specific activity of the enzymes SOD, catalase, glutathione reductase and glucose-6-phosphate dehydrogenase, aldehyde dehydrogenase and lactate dehydrogenase.

We showed the role of Na-BDP as an activator of the bactericidal and fungicidal action of the biocide benzalkonium chloride, despite the fact that Na-BDP does not exhibit an independent bactericidal and fungicidal effect. Na-BDP-benzalkonium chloride compositions in relation to *Aspergillus terreus*, *Penicillium chrysogenum* and *Paecilomyces variotii* were 20-30% more effective compared to pure benzalkonium chloride in a higher concentration.

In general, given the high antioxidant activity of Na-BDP nanoparticles with amino alcohols, the bactericidal and fungicidal action of Na-BDP nanoparticles with benzalkonium chloride, it can be assumed that the compositions with these components in a stable polymorphic form can be effective in the development of drugs for the treatment of skin diseases.

FUNDING

This research did not receive any specific grant from funding agencies in the public, commercial, or not-for-profit sectors.

ETHICS APPROVAL AND CONSENT TO PARTICIPATE

The animal study was conducted according to the guidelines of the Declaration of Helsinki and approved by the Local Ethics Committee of Privolzhsky Research Medical University, Russian Federation (protocol no. 1 from 18 January 2021). All efforts were made to minimize animal suffering and to reduce the number of animals used.

AUTHORS CONTRIBUTIONS

NM designed the article and wrote the manuscript. DM assisted in data visualization. IK and EA carried out chemical experiment. AS carried out biological experiment. All authors have reviewed, edited, and approved the final version of the manuscript.

CONFLICTS OF INTERESTS

The authors declare that they have no competing interests.

REFERENCES

1. Nicolov I, Georgescu D, Eftimie EL, Pinzaru SC, Roman R, Ambrus IL. DFT study of structure IR and raman spectra for betulinic acid solvatomorphs. Rev Chim. 2019 Feb;70(1):107-11. doi: 10.37358/RC.19.1.6861.
2. Wang X, Gong N, Yang S, Du G, Lu Y. Studies on solvatomorphism of betulinic acid. J Pharm Sci. 2014 Sep;103(9):2696-703. doi: 10.1002/jps.23853, PMID 24752825.
3. Yang D, Gong N, Zhang L, Lu Y. Isostructurality among 5 solvatomorphs of betulin: x-ray structure and characterization. J Pharm Sci. 2016 Jun;105(6):1867-73. doi: 10.1016/j.xphs.2016.03.015, PMID 27129904.
4. Yuki K, Ikeda M, Yoshida S, Ohno O, Suenaga K, Yamada K. Isolation of monovalerianester A, an inhibitor of fat accumulation from Valeriana fauriei. Nat Prod Commun. 2015;10(8):1333-4. doi: 10.1177/1934578X1501000806, PMID 26434106.
5. Zhang S, Peng B, Chen Z, Yu J, Deng G, Bao Y. Brain targeting acid-responsive antioxidant nanoparticles for stroke treatment and drug delivery. Bioact Mater. 2022 Mar 7;16:57-65. doi: 10.1016/j.bioactmat.2022.02.033, PMID 35386312.

6. Zhao X, Wang W, Zu Y, Zhang Y, Li Y, Sun W. Preparation and characterization of betulin nanoparticles for oral hypoglycemic drug by antisolvent precipitation. Drug Deliv. 2014 Sep;21(6):467-79. doi: 10.3109/10717544.2014.881438, PMID 24479653.
7. Pozharitskaya ON, Karlina MV, Shikov AN, Kosman VM, Makarov VG, Casals E. Pharmacokinetics and tissue disposition of nanosystem-entrapped betulin after endotracheal administration to rats. Eur J Drug Metab Pharmacokinet. 2017 Apr;42(2):327-32. doi: 10.1007/s13318-016-0340-7, PMID 27155877.
8. Chen X, Lu S, Gong F, Sui X, Liu T, Wang T. Research on the synthesis of nanoparticles of betulinic acid and their targeting antitumor activity. J Biomed Mater Res B Appl Biomater. 2022 Aug;110(8):1789-95. doi: 10.1002/jbm.b.35036, PMID 35179806.
9. Li Y, Wang Y, Gao L, Tan Y, Cai J, Ye Z. Betulinic acid self-assembled nanoparticles for effective treatment of glioblastoma. J Nanobiotechnology. 2022 Jan 21;20(1):39. doi: 10.1186/s12951-022-01238-7, PMID 35062946.
10. Amiri S, Dastghaib S, Ahmadi M, Mehrbod P, Khadem F, Behrouj H. Betulin and its derivatives as novel compounds with different pharmacological effects. Biotechnol Adv. 2020 Jan-Feb;38:107409. doi: 10.1016/j.biotechadv.2019.06.008, PMID 31220568.
11. Niewolik D, Dzido G, Jaszcz K. Studies on the preparation of nanoparticles from betulin-based polyanhydrides. Eng Proc. 2021 Oct 21;11(1):10. doi: 10.3390/ASEC2021-11160.
12. Gajbhiye SA, Patil MP. Breast cancer cell targeting of L-leucine-PLGA conjugated hybrid solid lipid nanoparticles of betulin vi a L-amino acid transport system-1. J Drug Target. 2025 May 14;33(8):1432-61. doi: 10.1080/1061186X.2025.2500036.
13. Chrobak E, Bebenek E, Kadela Tomanek M, Latocha M, Jelsch Ch, Wenger E. Betulin phosphonates; synthesis, structure and cytotoxic activity. Molecules. 2016 Aug 26;21(9):1123. doi: 10.3390/molecules21091123, PMID 27571057.
14. Bebenek E, Pecak P, Kadela Tomanek M, Orzechowska B, Chrobak E. Derivatives of betulin and betulinic acid containing a phosphonate group in silico studies and preliminary *in vitro* assessment of antiviral activity. Appl Sci. 2024 Feb 9;14(4):1452. doi: 10.3390/app14041452.
15. Chrobak E, Jastrzebska M, Bebenek E, Kadela Tomanek M, Marciniec K, Latocha M. Molecular structure *in vitro* anticancer study and molecular docking of new phosphate derivatives of betulin. Molecules. 2021 Jan 31;26(3):737. doi: 10.3390/molecules26030737, PMID 33572631.
16. Drag Zalesinska M, Kulbacka J, Saczko J, Wysocka T, Zabel M, Surowiak P. Esters of betulin and betulinic acid with amino acids have improved water solubility and are selectively cytotoxic toward cancer cells. Bioorg Med Chem Lett. 2009 Aug 15;19(16):4814-7. doi: 10.1016/j.bmcl.2009.06.046, PMID 19560351.
17. Tsepaeva OV, Nemtarev AV, Grigor'eva LR, Mironov VF. Synthesis of C^{28}-linker derivatives of betulinic acid bearing phosphonate group. Russ Chem Bull. 2021 Feb;70(1):179-82. doi: 10.1007/s11172-021-3074-x.
18. Melnikova NB, Malygina DS, Klabukova IN, Belov DV, Vasin VA, Petrov PS. Betulin-3,28-diphosphate physico-chemical properties and *in vitro* biological activity experiments. Molecules. 2018 May 14;23(5):1175. doi: 10.3390/molecules23051175, PMID 29757999.
19. Melnikova N, Malygina D, Panteleev D, Vorobyova O, Solovyeva A, Belyaeva K. The improvement of betulin-3, 28-diphosphate water-solubility by complexation with amines, meglumine and xymedon. Int J Pharm Pharm Sci. 2019 Apr 6;11(5):48-55. doi: 10.22159/ijpps.2019v11i5.32707.
20. Sirota TV. A novel approach to study the reaction of adrenaline autooxidation: a possibility for polarographic determination of superoxide dismutase activity and antioxidant properties of various preparations. Biochem Moscow Suppl Ser B. 2011;5(3):253-9. doi: 10.1134/S1990750811030139.
21. Aebi H. Catalase *in vitro*. Methods Enzymol. 1984;105:121-6. doi: 10.1016/s0076-6879(84)05016-3, PMID 6727660.
22. Sibgatullina GV, Khartendinova LR, Gumerova EA, Akulov AN, Kostyukova YA, Nikonorova NA. Methods for determining the redox status of cultured plant. Cells. Kazan: Kazan (Privolzhsky) Federal University; 2011.
23. Kochetov GA. Practical guide to enzymology. 2nd ed. Moscow: High School; 1980.
24. Solovyova AG, Zimin Yu V. A new estimation method of blood metabolism dynamics of patients with heat injuries. Mod Technol Med. 2012;12(2):116-7.
25. Guru SC, Shetty KT. Methodological aspects of aldehyde dehydrogenase assay by spectrophotometric technique. Alcohol. 1990 Sep-Oct;7(5):397-401. doi: 10.1016/0741-8329(90)90022-5, PMID 2222842.
26. Dawson JM, Heatlie PL. Lowry method of protein quantification: evidence for photosensitivity. Anal Biochem. 1984 Aug 1;140(2):391-3. doi: 10.1016/0003-2697(84)90183-0, PMID 6486427.
27. Xu J, Gilson DF, Butler IS. FT-Raman and high-pressure FT-infrared spectroscopic investigation of monocalcium phosphate monohydrate, $Ca(H_2PO_4)_2{\cdot}H_2O$. Spectrochim Acta A Mol Biomol Spectrosc. 1998 Oct;54(12):1869-78. doi: 10.1016/S1386-1425(98)00152-8.
28. Lien Vien D, Colthup NB, Fateley WG, Graselli JG, editors. The handbook of infrared and Raman Characteristic Frequencies of organic molecules. CA: Academic Press, Incorporated; 1991.
29. Quinone D, Veiga N, Torres J, Bazzicalupi C, Bianchi A, Kremer C. Self-assembly of manganese(II)-phytate coordination polymers: synthesis crystal structure and physicochemical properties. ChemPlusChem. 2017 May;82(5):721-31. doi: 10.1002/cplu.201700027, PMID 31961528.
30. Bartl F, Urjasz H, Brzezinski B. FT-IR study of pyridoxal phosphate. J Mol Struct. 1998 Jan 12;441(1):77-81. doi: 10.1016/S0022-2860(97)00282-2.
31. Youngme S, Phuengphai P, Chaichit N, Pakawatchai C, Van Albada GA, Roubeau O. The coordination chemistry of mono(di-2-pyridylamine) copper(II) complexes with monovalent and divalent oxoanions: crystal structure spectroscopic and magnetic properties of dinuclear $[Cu(L)(\mu\text{-}H_2PO_4)(H_2PO_4)]2$ and polynuclear $[Cu(L)(\mu3\text{-}HPO_4)]$. Inorg Chim Acta. 2004 Sep 10;357(12):3603-12. doi: 10.1016/j.ica.2004.04.027.
32. Nakamoto K. Infrared and Raman spectra of inorganic and coordination compounds part b, applications in coordination, organometallic and bioinorganic chemistry. 6th ed. New York: John Wiley & Sons, Inc; 2009.
33. Rodrigues Filho UP, Vaz S, Felicissimo MP, Scarpellini M, Cardoso DR, Vinhas RC. Heterometallic manganese/zinc-phytate complex as a model compound for metal storage in wheat grains. J Inorg Biochem. 2005 Oct;99(10):1973-82. doi: 10.1016/j.jinorgbio.2005.06.014, PMID 16054222.
34. Son LB. Synthesis of betulinic acid and development of its liposomal. In; Russian. Moscow; 1999.
35. McDonnell GE. Antisepsis disinfection and sterilization: types action and resistance. Washington, DC, USA: ASM Press; 2017. doi: 10.1128/9781555819682.
36. Gerba CP. Quaternary ammonium biocides: efficacy in application. Appl Environ Microbiol. 2015 Jan;81(2):464-9. doi: 10.1128/AEM.02633-14, PMID 25362069.
37. Barros AC, Melo LF, Pereira A. A multi-purpose approach to the mechanisms of action of two biocides (benzalkonium chloride and dibromonitrilopropionamide): discussion of *Pseudomonas fluorescens* viability and death. Front Microbiol. 2022 Feb 18;13:842414. doi: 10.3389/fmicb.2022.842414, PMID 35250955.
38. Li Z, Ma J, Ruan J, Zhuang X. Using positively charged magnetic nanoparticles to capture bacteria at ultralow concentration. Nanoscale Res Lett. 2019 Jun 4;14(1):195. doi: 10.1186/s11671-019-3005-z, PMID 31165285.
39. Draviana HT, Fitriannisa I, Jazidie A, Krisnawati DI, Khafid M, Kuo TR. Antibacterial mechanisms of negatively and positively charged ligands on gold nanoclusters. ACS Appl Nano Mater. 2025;8(13):6380-90. doi: 10.1021/acsanm.4c07269.